FRICTION-STIR WELDING OF ALUMINIUM ALLOY 5083

VARJENJE S TRENJEM IN MEŠANJEM ALUMINIJEVE ZLITINE 5083

Damjan Klobčar[1], Ladislav Kosec[2], Adam Pietras[3], Anton Smolej[2]

[1]Faculty of Mechanical Engineering, University of Ljubljana, Aškerčeva 6, 1000 Ljubljana, Slovenia
[2]Faculty of Natural Sciences and Engineering, University of Ljubljana, Aškerčeva 12, 1000 Ljubljana, Slovenia
[3]Instytut Spawalnictwa, Ul. Bł. Czesława 16/18 Gliwice, Poland
damjan.klobcar@fs.uni-lj.si

A study was made of the weldability of 4-mm-thick aluminium-alloy 5083 plates using friction-stir welding. A plan of experiments was prepared based on the abilities of a universal milling machine, where the tool-rotation speed varied from 200 r/min to 1250 r/min, the welding speed from 71 mm/min to 450 mm/min and the tool tilt angle was held constant at 2°. The factors feed per revolution (FPR) and revolution per feed (RPF) were introduced to get a better insight into the friction-stirring process. Samples for microstructure analyses, Vickers micro-hardness measurements and special miniature tensile-testing samples were prepared. The microstructure was prepared for observation on a light microscope under a polarised light source. A set of optimal welding parameters was determined at a FPR of 0.35 mm/r, at which quality welds can be made with a minimal increase in the weld hardness and an up to 15 % drop in the tensile strength.

Keywords: friction-stir welding, EN-AW 5083, welding parameters, mechanical properties, welding defects

Izdelana je študija varivosti 4 mm debele pločevine iz aluminijeve zlitine 5083 pri varjenju s trenjem in mešanjem. Načrt eksperimentov je bil pripravljen na podlagi sposobnosti univerzalnega frezalnega stroja. Spreminjali smo hitrost vrtenja orodja od 200–1250 r/min, hitrost varjenja 71–450 mm/min, kot nagiba orodja pa je bil konstanten pri 2°. Vpeljana sta bila faktorja podajanje na vrtljaj (FPR) in obratov na podajanje (RPF), s katerima bolj nazorno prikažemo vpliv parametrov procesa. Iz izdelanih varov smo pripravili vzorec za analizo mikrostrukture, vzorec za meritev trdote po Vickersu ter posebne miniaturne epruvete za natezni preizkus. Mikrostruktura je bila pripravljena za opazovanje na svetlobnem mikroskopu v polarizirani svetlobi. Optimalni parametri varjenja so bili ugotovljeni pri FPR 0,35 mm/r, pri čemer dobimo kakovostne zvare, z minimalnim povečanjem trdote vara in do 15-odstotnim padcem natezne trdnosti.

Ključne besede: varjenje s trenjem in mešanjem, EN-AW 5083, varilni parametri, mehanske lastnosti, napake v varu

1 INTRODUCTION

The 5083 aluminium alloy exhibits good corrosion resistance to seawater and the marine atmosphere, moderate mechanical properties and a high fatigue-fracture resistance. It has good formability, machinability and weldability using arc processes (metal inert gas – MIG or tungsten inert gas – TIG) or resistance welding.[1,2] This alloy is used for the production of welded components for shipbuilding and railway vehicles, different panels and platforms for boats and trains, storage tanks, cryogenics, pressure vessels, piping, tubing, welded tank trailers and welded dump bodies for the automotive industry, collapsible bridges, armour plates and the bodies of military vehicles. It can be subject to intercrystalline and stress-corrosion cracking after undergoing an unsuitable thermal treatment (welding). It should not to be used above 65 °C for an extended time if later exposed to a corrosive environment.[3] If the aluminium alloys are friction-stir processed (FSP) then superplastic properties are obtained, as a consequence of the grain refinement.[4–7] The surface of the aluminium alloys can be modified using shot pining and laser shot pinning, with a consequent influence on the microhardness, residual stresses, fatigue strength and corrosion resistance.[8–10]

Friction-stir welding (FSW) is a solid-state joining method that is energy and environmentally friendly and versatile. FSW joints have a high fatigue strength, require less preparation, and little post-weld dressing. These welds have fewer defects than fusion welds and the process enables the welding of dissimilar metals.[11] FSW has attracted significant research interest from industries like aerospace and transportation. Many studies were made on the weldability of 5083 aluminium alloy.[12–14] Some researchers studied the influence of FSW parameters on fatigue life.[12,14] They discovered that the rotational speed governs defect occurrence and a strong correlation between the frictional power input, the tensile strength and the low-cycle fatigue life is obtained. Han et al.[15] investigated the optimal conditions for FSW in correlation with welds' mechanical properties. These mechanical properties were similar to the base alloy at tool rotations between 500 r/min and 800 r/min at a weld-tool travel speed of 124 mm/min. Hirata et al.[16] investigated the influence of the FSW parameters on the grain size and the formability. They discovered that a decrease of the frictional heat flow during FSW

Table 1: Physical and mechanical properties of aluminium alloy 5083[3]

Property	ρ/kg m^{-3}	R_m/MPa	$R_{p0.2}$/MPa	E/GPa	T_{sol}/°C	T_{liq}/°C
AA5083-O	2.660	275–300	125–149	71	580	640

decreases the grain size, increases the ductility and improves the formability. Sato et al.[17] studied the influence of an oxide array on the formability of tailored blanks.[18] They discovered that a band of collective oxide particles could act as an initiation site for cracking during the forming processes. The research of Zucchi et al.[19] investigated the pitting and stress-corrosion cracking (PSCC) resistance of the 5083 aluminium alloy during FSW and MIG welding. The FSW welds showed better resistance to PSCC than the base alloy and much better resistance than MIG welds.

In this study the weldability of the 5083 aluminium alloy using friction-stir welding (FSW) was investigated. Welding parameters, i.e., the tool-rotation speed, the welding speed and the tilt angle have an influence on the formation of welding defects, the weld apices appearance, the microstructure and the weld strength. The aim of this research was to discover the welding parameters providing a weld microstructure without defects. The FSW employed a tool-rotation speed from 200 r/min to 1250 r/min, a welding speed from 71 mm/min to 450 mm/min and the tool-tilt angle was held constant at 2°. The factors feed per revolution (FPR) and revolutions per feed (RPF) were introduced to get a better insight into the friction-stirring process. The RPF gives information about the heat input per weld length. Miniature samples for tensile testing were prepared from the welds. The welds were examined under the light of an optical microscope and the Vickers hardness was measured.

2 EXPERIMENTAL

2.1 Dimensions and composition of the workpieces

The standard EN-AW 5083 aluminium alloy with chemical composition in mass fractions: 4.35 % Mg, 0.42 % Mn, 0.12 % Si, 0.087 % Cr, 0.29 % Fe, 0.019 % Zn, 0.013 % Ti and the rest Al, and temper O, was used for testing. The workpiece dimensions were 180 mm × 60 mm × 4 mm. The physical and mechanical properties of the alloy for temper O were not determined but taken according to the standard (**Table 1**).[3]
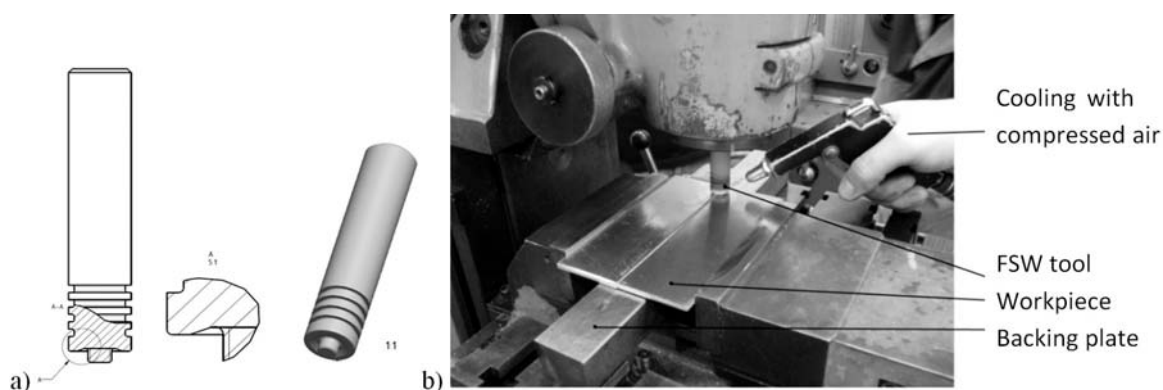
2.2 FSW tool

The FSW tool was made from standard EN 42CrMo4 steel[20]. A basic FSW tool geometry was used with a threaded pin that was 3.9 mm long (M6 × 1.5) and the concave shoulder (ϕ= 16 mm) for producing pressure under the tool shoulder (**Figure 1**).

2.3 Friction-stir welding

A plan of experiments was prepared regarding the capabilities of the universal milling machine used (Prvomajska ALG 100E). Different combinations of tool rotations and welding speeds were tested at a constant tilt angle of 2°. The FSW tool rotated from 200 r/min to 1250 r/min, and the welding speeds changed from 71 mm/min to 450 mm/min. The factors of feed per revolution (FPR) in μm/r and revolution per feed (RPF) in r/mm were introduced to better distinguish between the different welding parameters. The FPR varied from 56 μm/r to 2250 μm/r. RPF, which represents the "frictional heat input" per weld length, was between 17.6 r/min and 0.44 r/mm. A backing plate underneath the workpiece enabled the creation of pressure under the tool shoulder by preventing the aluminium alloy from flowing away from the seam. The two workpieces were clamped in a vice.

2.4 Preparation of samples and testing

From the FSW welds the miniature tensile test samples (**Figure 2**) were sectioned perpendicular to the

Figure 1: a) FSW tool geometry and b) experimental FSW
Slika 1: a) Geometrija orodja za FSW in b) potek eksperimenta FSW

welding direction, and weld cross-sections for analyses of the microstructure and the macrostructure were prepared. Before sectioning the samples with a water jet, the workpiece surfaces were milled to remove the weld underfill and the toe flash.
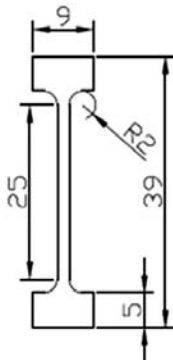
The uniaxial tensile tests were made using a computer-controlled Zwick/Roell Z050 tensile testing machine. The measurements were made using Testexpert software. The strain was measured with extensometer fixed directly on the sample.

The samples for analysis of the microstructure and microstructure were sectioned, grinded and polished. The samples for the macrostructure analysis were etched using Keller reagent (1125 mL HCl, 558 mL HNO$_3$, 200 mL HF and 1 500 mL H$_2$O) and the microstructure was analysed using an optical microscope. The samples for the microstructure analysis were anodized with Baker's reagent. The microstructure was examined using an optical microscope under polarised light and with a digital camera for acquiring the pictures. The Vickers micro-hardness HV1 (load equal to 9.807 N) was measured across the welds.
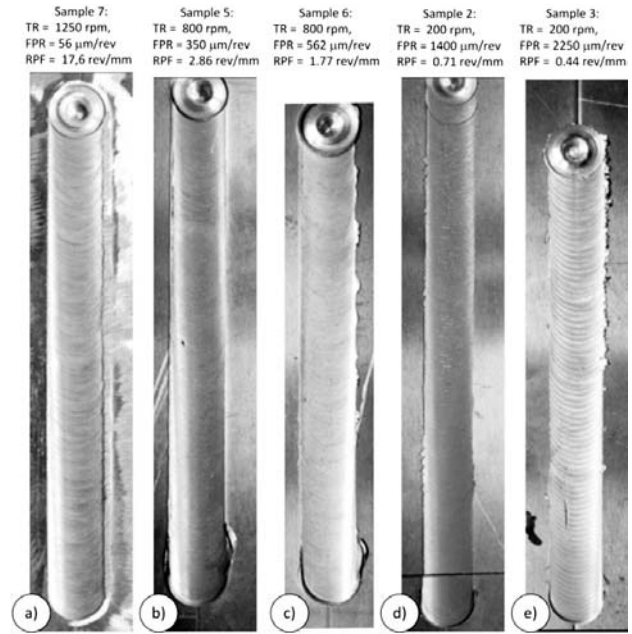
3 RESULTS AND DISCUSSION

3.1 Visual assessment of the FSW welds

Figure 3 shows a top view of the FSW welds. The end of the weld is indicated with a hole, which is a negative of the FSW tool pin. A visual assessment of the weld apices reveals smooth weld apices for FPR between 50 μm/r and 1000 μm/r, i.e., for a RPF between 20 r/min and 1 r/mm (**Figure 3**). For sample 7 (**Figure 3a**) the frictional heat input was the highest (RPF = 17.6 r/mm). For this sample the tool moved a little too much into the workpiece, due to the higher frictional heat input, which then softened the material. For samples 5 and 6 (**Figures 3b, c**) the RPF was 2.86 r/mm and 1.77 r/mm and the weld apices were smooth. When the tool speed was increased to a 0.71 r/mm and 0.44 r/mm (**Figures 3d, e**) the heat input become too small and the weld apices become rough with traces of material tearing.


Figure 3: A top view of the FSW welds
Slika 3: Pogled na temena FSW varov

The research of the influence of the width of the joint gap on the weldability showed that gaps wider than 0.5 mm could not be successfully welded, due to an inability to move the tool into the material to overcome the lack of material.

3.2 Weld microstructure

Macrographs of the selected FSW welds are shown in **Figure 4**. **Figure 4a** presents a macrograph of sample 7, which was welded with the highest frictional heat input

Figure 2: Drawing of miniature tensile test sample
Slika 2: Risba miniaturnega vzorca za natezni test
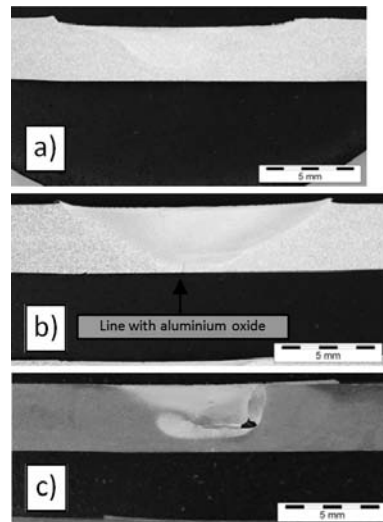
Figure 4: Macrostructure of FSW welds obtained at 200 r/min: a) sample 7 (FPR= 56 μm/r), b) sample 1 (FPR = 350 μm/r), c) sample 2 (FPR = 1400 μm/r) and c) sample 3 (FPR = 2250 μm/r)
Slika 4: Makrostruktura FSW varov, izdelanih pri 200 r/min: a) vzorec 7 (FPR= 56 μm/r), b) vzorec 1 (FPR = 350 μm/r), c) vzorec 2 (FPR = 1400 μm/r) in c) vzorec 3 (FPR = 2250 μm/r)

(RPF = 17.6 r/mm). The weld is without defects, except for possible under-fill, due to the higher heat input. A trace of the oxide line is present across the weld that was welded at 200 r/min and a 71 mm/min welding speed (FPR = 0.355 mm/r and RPF = 2.81 r/mm) (**Figure 4b**). The presence of Al_2O_3 on the surface of the touching planes in the weld joint before the welding is the reason for such a defect. This is why the oxide layer should be removed from the weld joint prior to welding. **Figure 4c** shows the FSW weld with a "worm hole" defect or "tunnelling" defect. This weld was produced at 200 rpm and a 280 mm/min welding speed (FPR = 1.4 mm/r and RPF = 0.71 r/mm). The "worm hole" defect appears if the welding is carried out with insufficient heat input or if the welding force in the axial direction is not large enough.

The weld microstructures on the top of the weld, inside the weld and at weld root are shown in **Figure 5**. The grain size is very small at the top of the weld (**Figure 5b**), which was in the vicinity of the tool shoulder. Small-sized grains are obtained across the whole weld (**Figure 5c**). At the weld root the material is not stirred to the bottom of the workpiece (**Figure 5d**). The oxide surface of contacting the workpieces is clearly seen as a line of oxides. Such an oxide line/layer could represent the initiation site for cracking during loading during forming or exploitation.

The analysis of the grain size showed that with a lower RPF, i.e., frictional heat input, the grain size decreases (**Figure 6**). For a higher frictional heat input the weld is heated well above the temperatures of recrystallization up to the temperatures where the grain growth takes place. When the RPF was 17.6 r/mm, the grain size of the weld and the base alloy were almost identical (**Figures 5** and **6a**). When the RPF was

Figure 6: Microstructure (polarised light microscopy images) of FSW weld produced at: a) 1250 r/min and RPF = 17.6 r/mm (sample 7), b) 200 r/min and RPF = 2.82 r/mm (sample 1), c) 1250 r/min and RPF = 2.78 r/mm (sample 0) and d) 200 r/min and RPF = 0.44 r/mm (sample 3)
Slika 6: Mikrostruktura (polarizirana svetlobna mikroskopija) FSW varov, izdelanih pri: a) 1250 r/min in RPF = 17,6 r/mm (vzorec 7), b) 200 r/min in RPF = 2,82 r/mm (vzorec 1), c) 1250 r/min in RPF = 2,78 r/mm (vzorec 0) in d) 200 r/min in RPF = 0,44 r/mm (vzorec 3)

approximately 2.8 r/mm, the grain size becomes approximately half the size of the base alloy (**Figures 6b, c**). The reason for this could be smaller heat input and the lower temperature of the workpiece. When welding with a RPF of 0.44 r/mm, the heat input was so low so that the stirring, i.e., cold deformations had a major role in grain refinement. In this case the grains were very small (**Figure 6c**) and the weld became harder.

3.3 Hardness

The Vickers hardness HV1 was measured across the weld in the middle of the weld (2 mm below the surface) over a total distance of 26 mm. The hardness is shown for the samples 7, 1, 0 and 3 (**Figure 7**). The centre of the weld is shown with the "dash-dot" line and the
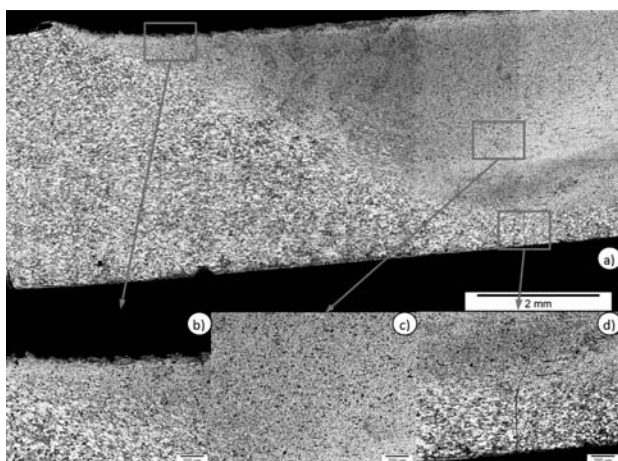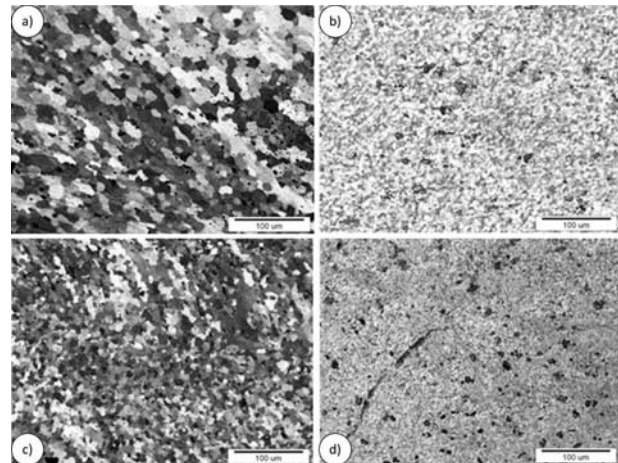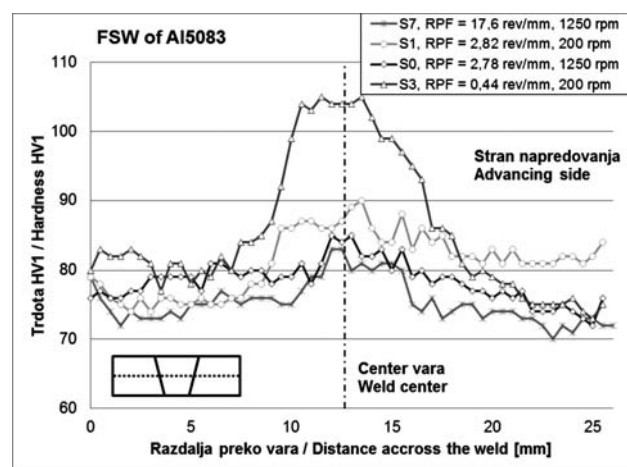

Figure 5: Microstructure (polarised light microscopy images) of FSW weld produced at 200 r/min FPR = 350 µm/r (sample 1): a) weld with HAZ and base alloy, b) weld apices and HAZ, c) weld and d) weld root
Slika 5: Mikrostruktura (polarizirana svetlobna mikroskopija) FSW vara, izdelanega pri 200 r/min in FPR = 350 µm/r (vzorec 1): a) var z TVP in osnovno zlitino, b) teme vara in TVP, c) var in d) koren vara

Figure 7: Hardness HV1 across the weld, HAZ and base alloy
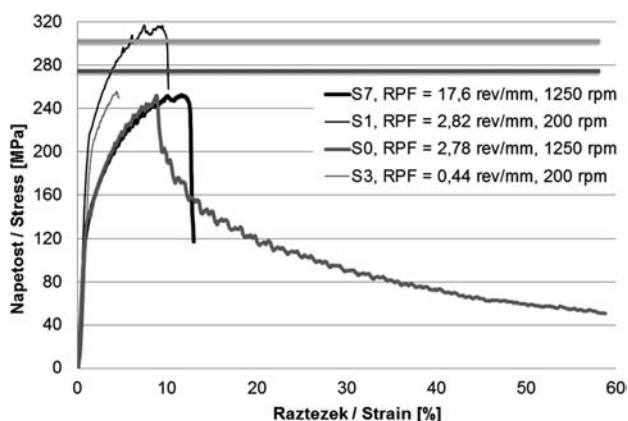**Slika 7:** Trdota HV1 preko vara, TVP in osnovnega materiala

Figure 8: Results of tensile tests
Slika 8: Rezultati nateznega testa

advancing side of the weld is on the right-hand side of the plot of **Figure 7**. When welding with a higher frictional heat input of 17.6 r/mm, the whole workpiece was heated above the temperature of recrystallization, where the grain growth occurs. The hardness was the lowest among all the compared samples ($\approx$74 HV1 in the base metal and HAZ, and 82 HV1 in the weld). When welding with optimal welding parameters (sample 0 and 1), the hardness across the weld was slightly higher ($\approx$84 HV1), similar to the base alloy where it was $\approx$80 HV1. A higher frictional heat input for the advancing side of the weld resulted in a lower hardness in the HAZ ($\approx$75 HV1). When the frictional heat input was very low ($\approx$0.44 r/mm) the weld hardness increased up to 105 HV1. Here, a deformational hardening was the dominating process due to a lower heat input. As a result of the higher frictional heat input on the advancing side of the weld, the hardness on the advancing side is generally lower than on the retreating side.

3.4 Tensile properties

The tensile strength of the base alloy used for the experimental workpiece was not measured for the experimental workpiece, but taken from the literature data (**Table 1**). The yield strength of the aluminium alloy 5083 is between 125 MPa and 149 MPa and the ultimate tensile strength between 275 MPa and 300 MPa (**Table 1**). Since non-standard test specimens were used, the results could not easily be compared with the results from the literature. The ultimate tensile strength of the tensile test specimens was generally in the range of the base aluminium alloy (**Figure 8**). When welding with 2.82 r/mm (sample 1), the tensile strength was even higher, i.e., 320 MPa. When welding with almost the same frictional heat input (sample 0), a strain at a tensile test of 60 % was measured, indicating the good potential for formability of the weld. When the heat input was low, i.e., the RPF was 0.44 r/mm, a strain of $\approx$5% was achieved as a consequence of the deformation-hardened microstructure.

4 CONCLUSIONS

Based on the analysed results the following can be concluded:

Smooth weld apices could be obtained when welding with an FPR between 50 μm/r and 1000 μm/r, i.e., for a RPF between 20 r/min and 1 r/mm.

When welding with the high frictional heat input ($\approx$20 r/mm): a) a risk of over-plunging and excessive flash generation is present, b) the stirred material heats well above the recrystallization temperature and the grain growth occurs, c) the hardness of the weld, the HAZ and the closer base alloy drops below the initial base-alloy hardness and d) an approximately 15 % lower tensile strength compared to the base alloy is obtained.

When welding with a medium heat input in the optimal range of welding parameters ($\approx$3 r/mm): a) the weld hardness increases slightly compared to the base alloy, b) the grains refine to half the size of the base alloy, due to the deformational hardening combined with the recrystallization, c) the weld has a higher tensile strength, and d) for higher tool rotations, a strain of around 60 % was measured, indicating the good forming potential of the weld.

When welding with a low heat input (RPF = 1 r/mm): a) the weld apices become rough and a tearing takes place, due to a too low frictional heat input, b) a "tunneling" or "elongated cavity" defect is usually present, c) the weld hardness increases since the deformation hardening becomes the dominating process, and d) an approximately 15 % lower tensile strength compared to base alloy is obtained.

A lower hardness was observed for the advancing side of the weld due to the slightly higher heat input compared to the retreating side.

5 REFERENCES

[1] J. Tušek, IEEE Trans. Plasma Sci., 28 (**2000**) 5, 1688
[2] P. Podržaj, I. Polajnar, J. Diaci, Z. Kariž, Science and Technology of Welding and Joining, 13 (**2008**) 3, 215
[3] http://aluminium. matter.org.uk/aluselect/
[4] A. Smolej, B. Skaza, B. Markoli, D. Klobčar, V. Dragojević, E. Slaček, Materials Science Forum, 706–709 (**2012**) 706, 395
[5] R. Mishra, Z. Ma, Materials Science and Engineering: R: Reports, 50 (**2005**) 1–2, 1
[6] Z. Ma, R. Mishra, Scripta Materialia, 53 (**2005**) 1, 75
[7] Z. Ma, S. Sharma, R. Mishra, Scripta Materialia, 54 (**2006**) 9, 1623

[8] U. Trdan, J. Grum, M. R. Hill, Materials Science Forum, 681 (**2011**) 480

[9] U. Trdan, J. L. Ocaña, J. Grum, Strojniški vestnik – Journal of Mechanical Engineering, 57 (**2011**) 05, 385

[10] S. Žagar, J. Grum, Strojniški vestnik – Journal of Mechanical Engineering, 57 (**2011**) 04, 334

[11] T. Debroy, H. K. D. H. Bhadeshia, Science and Technology of Welding & Joining, 15 (**2010**) 4, 266

[12] D. G. H. M. James, G. R. Bradley, International Journal of Fatigue, 25 (**2003**) 12

[13] D. Hattingh, C. Blignault, T. Vanniekerk, M. James, Journal of Materials Processing Technology, 203 (**2008**) 1–3, 45

[14] H. Lombard, D. Hattingh, A. Steuwer, M. James, Engineering Fracture Mechanics, 75 (**2008**) 3–4, 341

[15] S. J. L. Min-Su Han, J. C. Park, S. C. Ko, Y. B. Woo, S. J. Kim, Trans. Nonferrous Met. Soc. China, 19 (**2009**), 17

[16] T. Hirata, T. Oguri, H. Hagino, T. Tanaka, S. Chung, Y. Takigawa, K. Higashi, Materials Science and Engineering: A, 456 (**2007**) 1–2, 344

[17] Y. S. Sato, F. Yamashita, Y. Sugiura, S. H. C. Park, H. Kokawa, Scripta Materialia, 50 (**2004**) 3, 365

[18] J. Tušek, Z. Kampuš, M. Suban, J. Mater. Process. Technol., 119 (**2001**) 1/3, 180

[19] F. Zucchi, G. Trabanelli, V. Grassi, Materials and Corrosion, 52 (**2001**), 853

[20] Steel Selector Metal Ravne. 2012; Available from: http://www.metalravne.com/selector/steels/vcmo140.html